

## Research Article

## Open Access

László Himics, Sára Tóth\*, Miklós Veres, Péter Csíkvári, Margit Koós

# Influence of microwave plasma parameters on light emission from SiV color centers in nanocrystalline diamond films

**Abstract:** Zero phonon line (ZPL) shape, position and integral intensity of SiV defect center in diamond is presented for nanocrystalline diamond (NCD) films grown at different conditions. NCD films of average grain sizes from ~50 nm up to ~180 nm have been deposited onto c-Si wafer at substrate temperature of 700 and 850°C from mixture with different CH<sub>4</sub> and H<sub>2</sub> ratios using MWCVD process. Light emission of SiV defect center and Raman scattering properties of NCD samples were measured on a Renishaw micro-Raman spectrometer with 488 nm excitation. Scanning electron microscopy images were used for monitoring surface morphology and for the analysis of the average grain sizes. Sample thickness was determined by *in situ* laser reflection interferometry. Characteristics of SiV ZPL are discussed in light of the morphology, bonding structure and average grain size of NCD films.

**Keywords:** nanocrystalline diamond, MW CVD, SiV color center, photoluminescence, Raman scattering

DOI: 10.1515/chem-2015-0034

received January 31, 2014; accepted May 26, 2014.

## 1 Introduction

Formation, investigation and tailoring of color centers is one of the most intensely studied areas of diamond and nanodiamond (NCD) research nowadays due to

its favorable properties like biocompatibility, chemical stability and inertness. NCD with intentionally created light emitting color centers is a promising material for different high-tech applications, such as quantum technology [1-3], nanoscopy or nanoscale biomedicine [4]. The emission of different color centers related to impurities covers the whole spectral range from the deep ultraviolet to the far infrared. Thanks to their specific and unique properties – like single-photon emission, sensitivity to external influences and possibility of qubit creating, nitrogen and silicon related defect centers received much attention in last years. The silicon vacancy (SiV) center has a stable, intense and narrow zero-phonon line (ZPL) around 738 nm, which is right in the middle of the wavelength window of highest optical transparency of tissues [5], therefore diamond nanoparticles with SiV defects could be promising candidates for applications like *in vivo* biosensing. As a result of the weak electron-phonon coupling [6-8] its width (FWHM) has been found to be 5 nm at room temperature.

Silicon defects in diamond can be produced by the widely used ion implantation method [9] and also by incorporation during the growth process [10]. The latter is realized by introduction of Si atoms into the methane-hydrogen plasma, usually by sputtering of a Si wafer with the plasma itself. Obviously, the deposition parameters will have remarkable effect on both the properties of the grown nanodiamond films [11,12] and the incorporation of Si atoms, as well as on the formation of defect centers [13,14].

In this work the effect of precursor gas composition and substrate temperature on the spectral characteristics of SiV ZPL as well as on the emission intensity in nanocrystalline diamond films was investigated. Series of nanodiamond layers were prepared with different methane concentrations and substrate temperatures and the parameters like peak position, full width at half maximum (FWHM) and integral intensity of the SiV ZPL were correlated with the deposition conditions and features of

\*Corresponding author: Sára Tóth: Institute for Solid State Physics and Optics, Wigner Research Centre for Physics of the Hungarian Academy of Sciences, H-1525 Budapest, Hungary,  
E-mail: toth.sara@wigner.mta.hu

László Himics, Miklós Veres, Margit Koós: Institute for Solid State Physics and Optics, Wigner Research Centre for Physics of the Hungarian Academy of Sciences, H-1525 Budapest, Hungary

Péter Csíkvári: Department of Atomic Physics, Budapest University of Technology and Economics, H-1521 Budapest, Hungary

the structure. The aim of our work was to find the optimal deposition parameters giving material with high intensity, narrow, photostable SiV emission with small phonon side band in particle size as small as possible.

## 2 Experimental procedure

The samples were grown from a mixture of  $\text{CH}_4$  and  $\text{H}_2$  using microwave chemical vapor deposition (2.45 GHz), where Si wafers served as substrates through the bias-enhanced nucleation and growth process, where the chamber pressure was kept at 40 mbar and the microwave power was 1200 W. The total gas flow in each case was 100 sccm. The generation of diamond grains on the substrate surface was done with 4% methane ratio and 200 V bias voltage for 30 minutes. The deposition process was performed at different methane concentration being the methane ratio of 0.2, 0.5, 1 and 2% in the source gas, while the substrate temperature was 700 and 850°C. The growth process was holding for 2 hours in each case. The layer thickness was determined by laser reflection interferometry used as in situ measurements.

PL and Raman spectra were recorded on a Renishaw 1000 Raman spectrometer attached to a Leica DM/LM microscope. The 488 nm line of an Ar-ion laser served as excitation source for both types of measurements. The excitation beam was focused into a spot having diameter of 1 micron and its power on the sample surface was around 10 mW.

Morphology of the samples was investigated with a LEO 1540XB FIB workstation. The average grain size of CVD films was determined by two methods. In first case the ImageJ software was used, which is a free computer program to processing different type of images. This software is able to count the number of grains or particles and determine their size on the predetermined area of analyzing picture and finally estimates the average grain size. The good quality of picture and a carefully selected threshold is critical for the obtained result. In second case we used a simple, manual way to estimate the average grain sizes. We controlled the results manually with a specified approximate threshold, because the adjustment of this value in this software has a great effect to the obtained grain size, which could give an unreal distribution. A straight line was drawn on each SEM picture with 1 micron length. To confirm, the length of the lines drawn on the pictures was used with the scale displayed previously by the original SEM software. The length was divided by the number of grains lie on the line and was determined

the average grain size. The above-described process was repeated in three different areas for each picture to estimate average grain sizes of the NCD film.

## 3 Results and discussion

In the case of CVD growth diamond films, the substrates usually are non-diamond layers. We have used silicon wafer, so the first step in the growth process is the nucleation of diamond. Many techniques have been used, but the bias-enhanced nucleation could result the highest nucleation density in the surface of the substrate [15]. After the nucleation diamond nuclei could grow three dimensionally until they coalesce and form continuous film. After the coalescence, it grows epitaxially on the individual diamond crystal faces depending on the quality, doping and degree of bulk defects determined by the growth chemistry (gaseous carbon species and dopant concentration). Through this process non-diamond carbon species could grow and form intergrain structures in the film. Temperature and growth chemistry are key parameters in the aspect of growth rate and growing crystalline texture.

Fig. 1 shows typical SEM micrographs of the nanodiamond samples prepared, corresponding to lowest and highest methane concentrations used at two substrate temperatures. It can be seen that the methane concentration has a remarkable effect on the grain size of the formed films. Diamond crystallites can be recognized in all of the samples with significant differences in the morphology. Films prepared at 700°C substrate temperature (Figs. 1a, 1b) have more uniform grain size distribution, with some cauliflower pattern observable for the samples obtained with 2.0%  $\text{CH}_4$  concentration, characteristic for ultrananocrystalline diamonds.

SEM micrographs of films prepared at 850°C (Figs. 1c, 1d) exhibit different orientation texture of crystallites for both samples prepared with 0.2 and 2%  $\text{CH}_4$  concentration. Beside the growth chemistry the surface temperature determines the relative growth rate of individual crystal faces, the faster growing facets will overgrow slower growing hence the growing film takes on the orientation texture of the crystallites [16]. The average grain size is larger for 0.2% and nearly the same for 2% methane concentration compared to the films prepared at 700°C substrate temperature.

Average grain sizes determined by two different methods (see details in Experimental section) are shown on Fig. 2. for sample series prepared at 700°C and 850°C

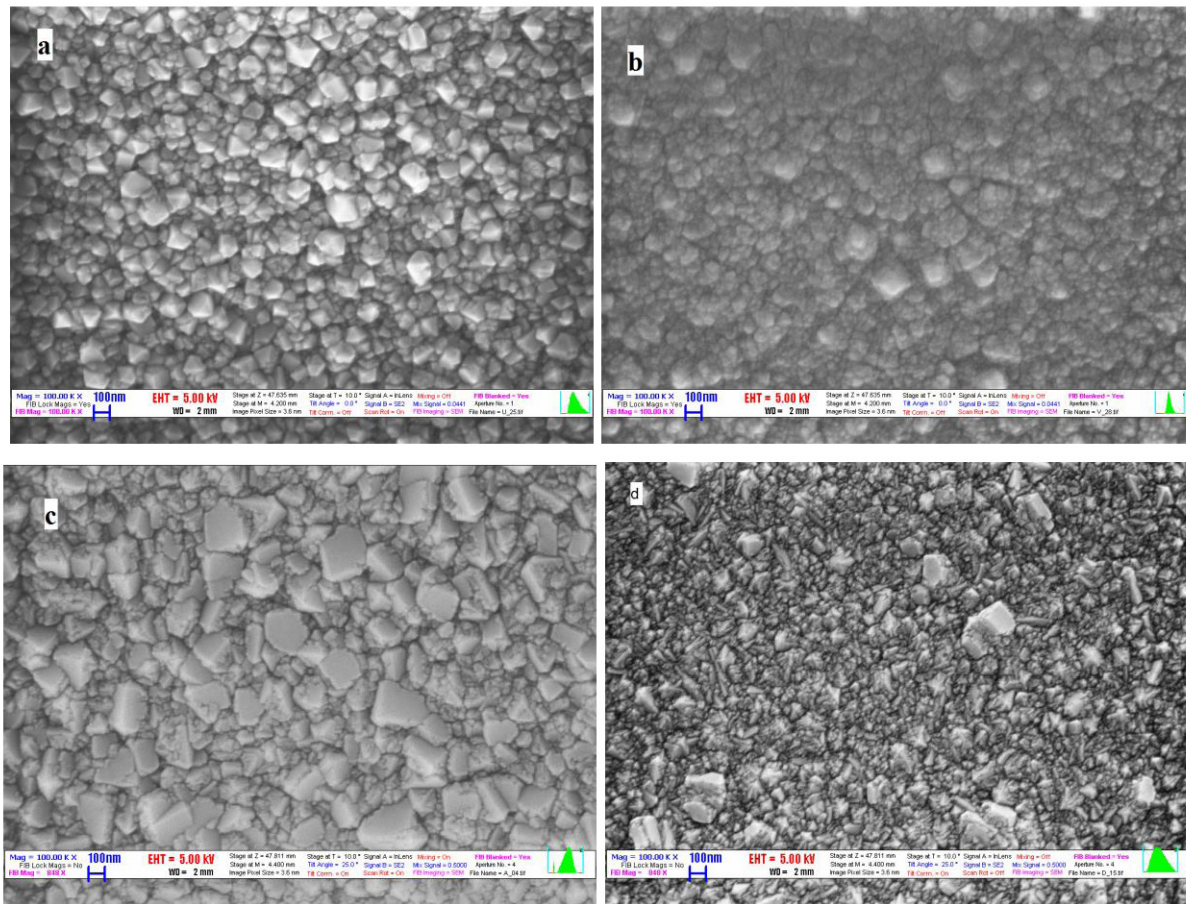


**Figure 1:** SEM micrographs of NCD thin films prepared at (a)  $T=700^{\circ}\text{C}$  and  $0.2\% \text{CH}_4$ ; (b)  $T=700^{\circ}\text{C}$  and  $2.0\% \text{CH}_4$ ; (c)  $T=850^{\circ}\text{C}$  and  $0.2\% \text{CH}_4$  and (d)  $T=850^{\circ}\text{C}$  and  $2.0\% \text{CH}_4$ .

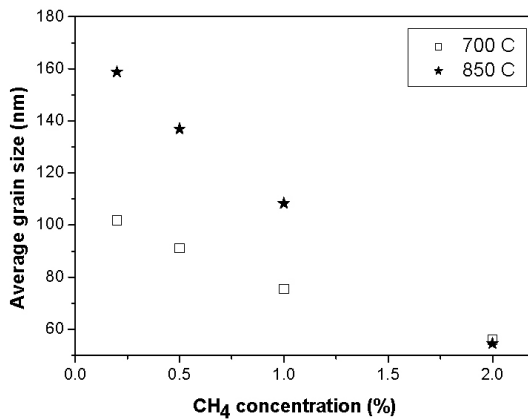


**Figure 2:** Average grain size of the NCD films prepared under different conditions.

substrate temperatures. We have obtained characteristic dependence for both series: the average grain size

decreases as the methane concentration in the source gas increases. At the same time the substrate temperature has significant influence on the average grain sizes, the higher the substrate temperature, the larger the average grain sizes can be observed, except for 2% methane concentration. It is interesting to mention that the average grain size and layer thickness (see Figs. 2 and 3) for the films prepared with 0.2%  $\text{CH}_4$  are close.

The evolution of the Raman spectra with methane concentration for sample series grown at two different substrate temperatures is shown on Fig. 3. All spectra were normalized to the G-band and shifted along the ordinate for the better visibility. The presented spectra are typical for NCD films grown on Si substrate and contain peaks that can be assigned to c-Si Raman scattering and oxygen contamination on NCD films. Relatively weak and broad band at  $950\text{-}1000\text{ cm}^{-1}$  is related to the second-order Raman scattering of crystalline Si substrate [17].

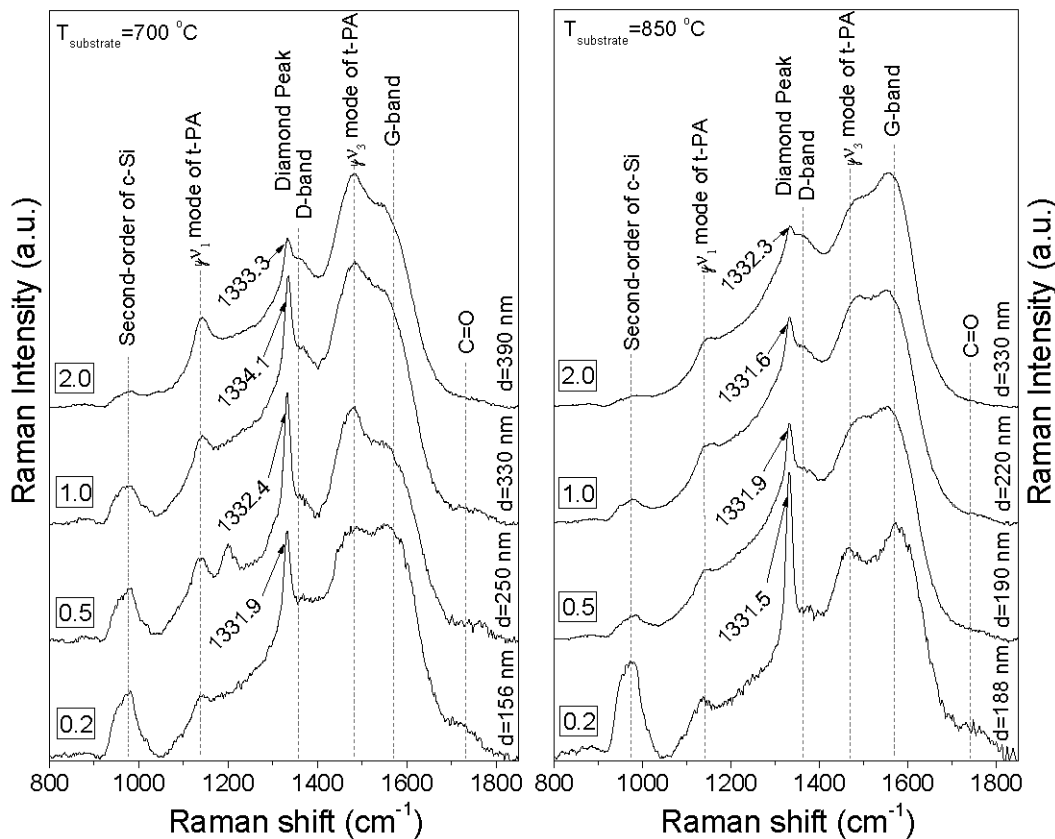


Figure 3: 488 nm excited Raman spectra of the NCD films prepared under different conditions.

The presence of above-mentioned peak in spectra could demonstrate the transparency of diamond films for 488 nm excitation wavelengths as well as for the scattered light of Si wafer. The perfect diamond crystal is transparent in this wavelength region and the observed decreasing tendency in the transparency indicates the increase of non-diamond component in the samples. Worthy of note that the transparency in the c-Si second-order Raman scattering region decreases more slowly with methane concentration of source gas for series prepared at 700°C compared to series prepared at 850°C. It is in good accordance with relative intensification of G-band scattering with methane concentration for films of 850°C.

Nanodiamond films consist of diamond crystallites, an amorphous intergrain phase and the interface between the two above, the so called grain boundaries. The corresponding Raman scattering bands are the diamond peak, the D and G bands and the nanodiamond fingerprint peaks in the Raman spectrum, respectively. The characteristic diamond peak (Brillouin zone-center  $T_2g$  mode at  $1332\text{ cm}^{-1}$ ) is clearly evident in all spectra.

Its position depends on the magnitude of the residual strain, which is always present in diamond film, and changes from  $1331.9$  to  $1334.1\text{ cm}^{-1}$  for sample series deposited at 700°C and from  $1331.5$  to  $1332.3\text{ cm}^{-1}$  for sample series prepared at 850°C substrate temperature. Shifting of the diamond Raman line position in NCD film compared to the stress-free, single crystal is the result of the sum of different stresses. Several stress sources, like the different thermal expansion coefficient of Si substrate and diamond, the misfit of diamond and silicon crystal lattice as well as the internal stress, assign to different impurities and structural defects produced under growth process, create a residual stress, which has impact on the diamond Raman line shift. While the compressive stress induces shifting of diamond Raman line to higher frequency, the tensile causes shift to lower respectively.

Based on the Raman spectra the influence of substrate temperature and  $\text{CH}_4$  concentration of source gas have impact on the bonding properties and microstructure of the forming films. In spectra measured on samples

deposited at 700°C the higher methane concentrations result in relative decrease of G peak intensity and relative enhancement of the nanodiamond fingerprint bands (1140 and 1470 cm<sup>-1</sup>). These peaks usually appear in Raman spectrum of nanosized diamond simultaneously and were assigned to the  $v_1$  and  $v_3$  modes of trans-polyacetylene [18]. Increasing methane concentration results in smaller grains with ordered grain boundaries and less intergrain amorphous carbon. In case of the higher deposition temperature (850°C) the relative increase of the G and D peaks intensity and relative decrease of the fingerprint peaks can be observed. The G-peak is related to the stretching vibration of the sp<sup>2</sup> C-C bonds (rings and chains); the D-band is in connection with the breathing mode of the sp<sup>2</sup> carbon containing rings. The series prepared at higher substrate temperature with increasing methane concentration features larger grains (Fig. 2), less ordered grain boundaries and higher disordered carbon content compared to the series prepared at lower temperature. Concerning the grain size of 2% CH<sub>4</sub> sample is unique in this respect. For both sample series the relative decrease of Raman peak intensity with increase of CH<sub>4</sub> concentration can be due to graduated increase of sp<sup>2</sup> content in samples which, because of large scattering cross-section, dominates Raman scattering.

The variation of bonding properties and morphology with deposition conditions presages their influence to the SiV emission features, too. Silicon is frequently incorporated into CVD diamond films due to the etching of silicon substrate and silicon-containing growth chamber components. Clark and Dickerson [19] found that if the deposition plasma is in direct contact with the quartz reactor walls this process might even become the main Si source. In our deposition process the incorporation of Si foreign atoms into growing films takes place in a similar way. The deposition time was the same for every films, however the different growth rate due to the different deposition condition, results in different silicon concentration sputtered from the substrate. This departure in silicon concentration as plasma can be compensated from the sputtering of the quartz reactor walls, so silicon can be incorporated into growing surface.

Fig. 4 shows the 488 nm excited PL spectra in the region of the SiV-related peak for two sample sets, corresponding to 700°C and 850°C substrate temperatures, respectively. The observed peak position around 738 nm and the weak vibronic band on long wavelength side of the spectrum, corresponding to phonon replica of the ZPL, are typical features of the SiV emission. Comparison of the emission of two sets of samples shows that the evolution of the PL band with methane concentration takes place differently.

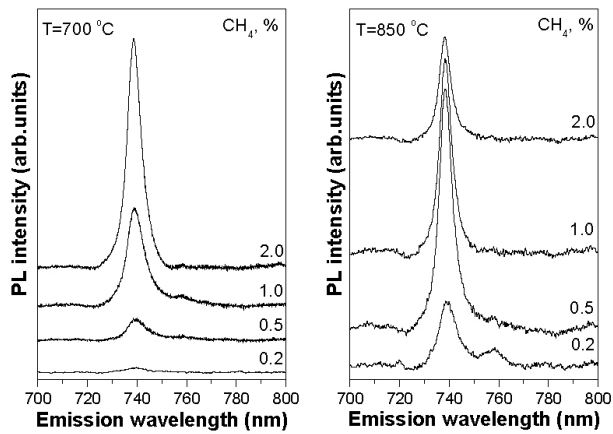


**Figure 4:** SiV peak region in the photoluminescence spectra of NCD films prepared at 700°C and 850°C substrate temperatures from gas mixtures of different methane content. The excitation wavelength is 488 nm.

The increasing methane ratio results in constant increase of the SiV peak intensity in case of sample set prepared at 700°C. Considering the emission spectrum of the other sample set grown at 850°C, it has an upside U-shape dependence on methane concentration. In the 850°C sample, the highest intensity corresponds to 0.5% methane concentration and it decreases for both smaller and higher CH<sub>4</sub> concentrations. To see the exact changes in the PL spectral shape caused by the increasing methane concentration, fitting parameters of the SiV ZPL were depicted in Fig. 5.

In sample prepared at 700°C and 0.2% CH<sub>4</sub> concentration the ZPL of the SiV is located at 739.4 nm with 10.2 nm FWHM (see □ in Fig. 5.), which is quiet far from the “ideal” SiV (peak at 738 nm with FWHM about 5 nm) emission. It can be seen that as CH<sub>4</sub> concentration increases, both the position (738.9 nm) and width (6.9 nm) of the SiV PL peak decrease. In case of samples grown at 850°C and 0.2% methane concentration the ZPL is found to be at 739.4 nm and its FWHM is 8.6 nm. The descending tendency in the peak position and the broadening of the SiV ZPL with methane concentration could be observed in this case too, hence the emission characteristics are tend to be closer to the theoretical predicted values.

From comparison of spectral characteristic determined for the two series can be established: i) pronounced change in the ZPL parameters of SiV defect center in diamond takes place when the CH<sub>4</sub> content of source gas increases from 0.2% to 0.5% for both series; ii) the broadening of SiV ZPL is larger for every NCD films prepared at 700 °C substrate temperature compared to ones deposited at 850°C; iii) the best parameters characterizes of SiV ZPL

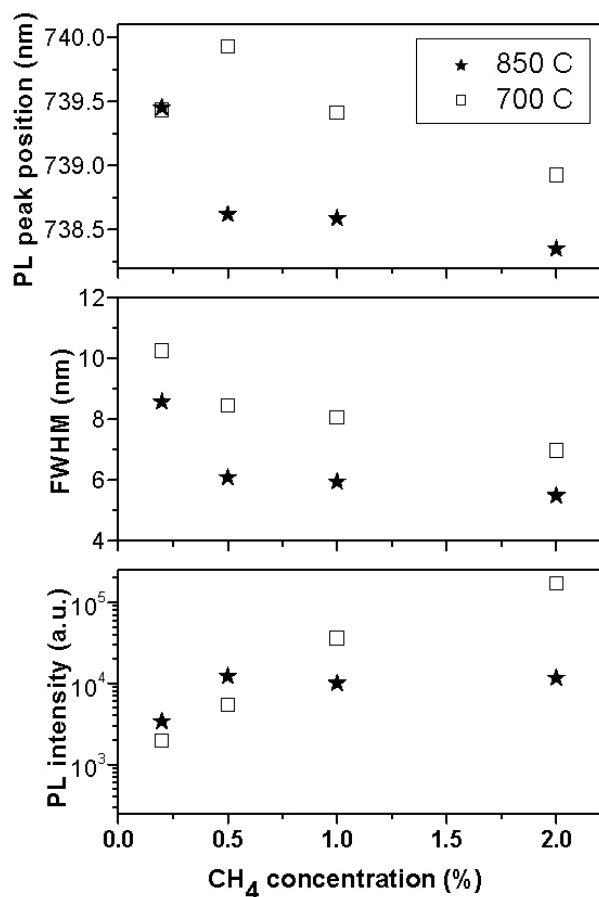


**Figure 5:** Evolution of SiV PL peak parameters with methane content of the feed gas in sample sets prepared at different substrate temperatures. The emission intensity is normalized to diamond Raman peak intensity obtained from the multicomponent fitting of the Raman spectra measured on the given sample. Small increase of luminescence intensity with methane concentration can be established for sample series prepared at 850°C and more significant increase of light emission can be seen for sample series prepared at 700°C. An exact result for emission intensity could be obtained by the correction for absorption coefficient, which determination is in progress. Although the Raman scattering spectra shown on Fig. 4 exhibits more graphitic structure for sample series of 850°C, which could enhance the optical absorption of emitted light and hence self-absorption contributes to intensity decrease for this sample series.

the NCD films grown at 850°C with 0.5, 1 and 2% methane concentration of source gas.

The atomic structure of SiV consists of a silicon atom splitting two vacancies as was recently confirmed by EPR measurements [20]. For the formation of SiV defect center the silicon incorporated from the plasma and carbon vacancy formed in growing films should diffuse to incorporated silicon. This very simple picture gives some background to explain difference in SiV ZPL parameters in the case of two deposition temperatures. To initiate vacancy diffusion in NCD films high temperature (800°C) annealing is needed. In this aspect substrate temperature of 850 °C is more favorable for the formation of complex SiV defect center and for the relaxation of its surroundings. For NCD sample series deposited at 700°C substrate temperature an incomplete relaxation takes place in the vicinity of SiV complex therefore the local strain imposed on the defect

exhibits some distribution. This is the reason why the SiV ZPL parameters exhibit more difference compared to theoretical values.

A considerable broadening and shift of ZPL peak position to longer wavelengths for NCD films prepared at 0.2% methane concentration at both substrate temperatures can also be related to strain effect. For this methane concentration the growth rate is small, the thin layer thickness is comparable to average grain size (see Figs. 3 and 4). The strain caused by silicon substrate in this thin layer could be more effective compared to more thick films and results in large difference in ZPL parameters. As the methane concentration increases the growth rate also increases until its saturation (~2% CH<sub>4</sub>) and the growing NCD layer thickens. Parallel with this process the change of ZPL parameters “saturates” too. The homogeneous and inhomogeneous broadening of SiV ZPL will be analyzed later to get more information for the influence of local strain.

Let us consider the integral intensity of SiV ZPL shown on Fig. 5. The emission intensity is normalized to diamond Raman peak intensity obtained from the multicomponent fitting of the Raman spectra measured on the given sample. Small increase of luminescence intensity with methane concentration can be established for sample series prepared at 850°C and more significant increase of light emission can be seen for sample series prepared at 700°C. An exact result for emission intensity could be obtained by the correction for absorption coefficient, which determination is in progress. Although the Raman scattering spectra shown on Fig. 4 exhibits more graphitic structure for sample series of 850°C, which could enhance the optical absorption of emitted light and hence self-absorption contributes to intensity decrease for this sample series.

## 4 Conclusions

The dependence of the SiV photoluminescence features on substrate temperature and CH<sub>4</sub>/H<sub>2</sub> ratio were analyzed in correlation with structural properties of CVD-grown nanodiamond layer. It was found that the methane content, as well as the grain size has a leading role in the formation of the SiV color center. The methane content affects the SiV PL emission intensity, while substrate temperature affects the peak position and widths. While the use of 850°C will favor the more ideal emission features of SiV, smaller temperature will lead to SiV emission of higher intensity.

**Acknowledgement:** This work was supported by the Hungarian Science Foundation under contract number OTKA PD-106130.

## References

- [1] Kurtsiefer C., Mayer S., Zarda P., Weinfurter H., *Phys. Rev. Lett.*, 2000, 85, 290
- [2] Beveratos A., R. Brouri, Gacoin T., Willing A., Poizat J.P., Grangier P., *Phys. Rev. Lett.*, 2002, 89, 187901
- [3] Jelezko F., Gaebel T., Popa I., Domhan M., Gruber A., Wrachtrup J., *Phys. Rev. Lett.*, 2004, 93, 130501
- [4] Ho D. (Ed.), *Nanodiamonds, Applications in Biology and Nanoscale Medicine*, Springer, New York, 2010
- [5] Chance B., Cope M., Gratton E., Ramanujam N., Tromberg B., *Review of Scientific Instruments*, 1998, 69(10), 3457
- [6] Wang C., Kurtsiefer C., Weinfurter H., Burchard B., *J. Phys. B*, 2006, 39, 37
- [7] Vlasov I.I., Barnard A.S., Ralchenko V.G. et al., *Adv. Mater.*, 2009, 21, 808
- [8] Gaebel T., Popa I., Gruber A., Domhan M., Jelezko F., Wrachtrup D., *New J. Phys.*, 2004, 6, 98
- [9] Wang C., Kurtsiefer C., Weinfurter H., Burchard B., *J. Phys. B: At. Mol. Opt. Phys.*, 2006, 39, 37
- [10] Sedov V.S., Vlasov I.I., Ralchenko V.G., Khomich A.A., Konov V.I., Fabbri A.G., Conte G., *Bull. Lebedev Phys. Inst.*, 2011, 38, 291
- [11] May P.W., Ashfold M.N.R., Mankelevich Yu.A., *J. Appl. Phys.*, 2007, 101, 053115
- [12] Borges C.F.M., Moisan M., Gicquel A., *Diam. Rel. Mat.*, 1995, 4, 149
- [13] Locher R., Wild C., Herres N., Behr D., Koidl P., *Appl. Phys. Lett.*, 1994, 65, 34
- [14] Nistor S.V., Stefan M., Ralchenko V., Khomich A., Schoemaker D., *J. Appl. Phys.* 2000, 87, 8741
- [15] Yugo S., Kanai T., Kimura T., Muto T., *Appl. Phys. Lett.*, 1991, 58, 1036
- [16] Butler J.E., Sumant A.V., *Chem. Vap. Dep.*, 2008, 14, 146
- [17] Mishra P., Jain K.P., *Phys. Rev. B*, 2001, 64, 073304
- [18] Brillante A. et al., *Physica*, 1986, 139, 533
- [19] Clark C., Dickerson C., *Surf. Coat. Tech.*, 1991, 47, 336
- [20] Edwards A.M., Newton M.E., Martinean P.M., Twitchen D.J., Williams S.D., *Phys. Rev. B*, 2008, 77, 245205